Application of the Phase Doppler Measurement Technique for the Characterization of Supersonic Gas Atomization

Niklas Apell*, Cameron Tropea, Ilia V. Roisman, Jeanette Hussong

Institute for Fluid Mechanics and Aerodynamics, Technische Universität Darmstadt, Germany
*Corresponding author: apell@sla.tu-darmstadt.de

Keywords: phase Doppler measurement technique, supersonic gas atomization

ABSTRACT

A dual-mode phase Doppler measurement system has been set up for the characterization of the complex spray produced through supersonic gas atomization. The atomizer design has been based on a generic close-coupled configuration operated with water and air, which leads to high local Mach numbers and complex patterns of compression and expansion waves within the gas flow field. As a result, the dense spray is characterized by high particle velocities and a wide range of particle sizes, which proves challenging for experimental investigations.

Measurements of local particle size and velocity distributions have been performed in various radial positions within the spray downstream of the atomizer, where the spray is fully developed. The set point of operation, which is defined by the gas stagnation pressure and the liquid mass flow rate, has been varied systematically, covering a wide range. By decoupling both operational parameters, their influence on the atomization result has been investigated independently. Furthermore, the atomizer geometry has been varied in terms of liquid nozzle diameter and liquid nozzle protrusion length.

In accordance with data from the literature, the gas stagnation pressure has been observed to lead to decreasing median particle size and dispersion of the particle size, when increased. However, as a novel finding, the atomization result has been shown to be more sensitive to changes in the liquid mass flow rate. Thus, increasing the liquid mass flow rate results in an increase in both the median particle size and the dispersion of the particle size. The relationship between the atomization result and the gas-to-liquid ratio has been clearly shown to be ambiguous, that is, a function of the gas stagnation pressure and the liquid mass flow rate.

Neither the liquid nozzle diameter nor the liquid nozzle protrusion length have been found to have an influence on the median particle size. However, the latter clearly influences the dispersion of the particle size in a complicated way, while the effect of the liquid nozzle diameter is more subtle. It has been concluded that the complex coupling between operational parameters and the specific atomizer design evident in supersonic gas atomization requires a deeper understanding of the local gas flow field and its interaction with the liquid flow.

1. Introduction

The atomization of liquids by means of supersonic gas flows is extensively used in numerous industrial applications, especially in metal processing. Common examples are the production of fine

metal powders used in additive manufacturing as well as spray deposition as a near net shape manufacturing process (Henein et al., 2017). Although economic interest in these applications is growing, understanding of the physical mechanisms involved in supersonic gas atomization and their predictive modeling capabilities are still limited. One reason for this shortcoming is a lack of comprehensive experimental data providing insight into the influence of operational parameters on the atomization result, specifically, the local particle size distribution. Indeed, experimental studies of supersonic gas atomization are extremely difficult due to three main reasons. First, the length scales of the resulting particles can be very small and still span a range of two orders of magnitude. Second, the high gas velocities of up to several hundred meters per second lead to very fast particles and, therefore, very short time scales. Third, the resulting sprays are often very dense, further limiting the choice of suitable measurement techniques.

Consequently, available experimental data is mostly based on the subsequent analysis of powders produced by means of supersonic gas atomization employing, for instance, image analysis or sieving. Selected examples for this approach are Mates and Settles (2005), Anderson and Terpstra (2002), Ünal (2006, 2007a, 2007b), Aksoy and Ünal (2006) and Ünal and Aydın (2007). Probably the most extensive study of this kind to date is the one reported on by Urionabarrenetxea et al., 2021, covering a wide range of set points of operation as well as several different molten metals, gases and atomizer designs. In general, the results of these studies have been used to identify trends with regard to the influence of operational parameters on the atomization result. For instance, the particle size is commonly found to decrease with increasing gas stagnation pressure. However, analyzing raw powders as a means for assessing the atomization process has several shortcomings. On the one hand, this approach does not provide insight into local particle size and velocity distributions within the spray, which is crucial information for understanding and, possibly, influencing the atomization mechanisms. On the other hand, the powders are the integral result of the atomization process, taking place over a finite time interval. Therefore, the effect of fluctuations of the set point of operation on the particle size cannot be identified. This is especially important, since in many supersonic gas atomization processes the liquid is gravity driven, resulting in, for instance, a time-dependent liquid mass flow rate, which decreases with decreasing liquid level. As has been shown by Allimant et al. (2009) using a time-dependent sampling system, this has a significant influence on the temporal development of the particle size.

In contrast, the phase Doppler measurement technique, providing a non-invasive means for investigating local particle size and velocity distributions, has been employed by few authors. For instance, Wolf and Bergmann (2002) have set up a phase Doppler measurement system described by Domnick et al. (1997) and Domnick et al. (1998) for the on-line process monitoring of an atomizer used for the production of metal powders. They have obtained radial profiles of mean particle size and velocity for varying fluid mass flow rates and liquid properties, successfully demonstrating the suitability of the measurement technology for the application in supersonic gas atomization. However, due to the complexity of supplying liquid metal to the atomizer and the strong coupling between gas and liquid flow as well as atomizer geometry, they have reported difficulties in keeping a constant set point of operation, that is, liquid mass flow rate and temperature. A systematic

study has been attempted by, for instance, Antipas (2011), who has performed radially resolved measurements in a water spray using different atomization gases. For the results, however, no well-defined set point of operation has been reported.
In the present experimental study, a commercially available phase Doppler measurement system has been set up and employed to measure local particle size and velocity distributions in a water spray produced by a generic close-coupled atomizer operated with air at well-defined set points of operation. These measurements were used to study the influence of operational parameters as well as the atomizer geometry on the atomization result in terms of local particle size and velocity distributions.

2. Experimental setup and methods

In the following, a brief overview of the atomizer research facility, including the covered parameter range, is given. Next, the setup of the phase Doppler measurement system is described. Finally, the methods used for the experimental data acquisition as well as the data post-processing are introduced.

2.1. Close-coupled atomizer research facility

The atomizer used in this experimental study is based on a close-coupled configuration and has been operated with water and air as working fluids. It consists of a central liquid nozzle, surrounded by a single coaxial gas nozzle featuring an annular slit design. Characteristic for the close-coupled configuration is the close proximity of liquid and gas nozzle, promoting the strong interaction of the two fluids. A schematic illustration of a generic close-coupled atomizer as commonly used for the production of metal powders is shown in Fig. 1a.

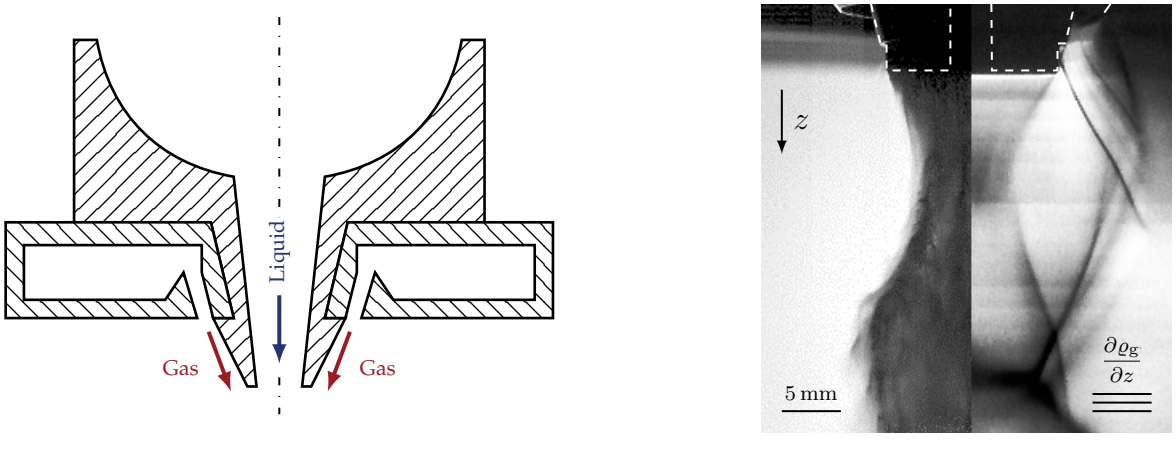

(a) (b)

Figure 1. Close-coupled atomizer configuration: a) schematic illustration (adapted from Apell et al. (2021)), and b) exemplary flow-field visualized using high-speed imaging (left, multi-phase flow) and focusing Schlieren imaging (right, gas-only flow, as described by Luh et al. (2018)).

The gas nozzle is connected to a high pressure supply line capable of providing up to $18\,\mathrm{m}^3$ of air at a pressure of approximately $3.5\,\mathrm{MPa}$. It features a convergent-divergent design, producing an exit Mach number of about $Ma = 1.2$. For a gas stagnation pressure of $p_{\mathrm{t,g}} \approx 0.26\,\mathrm{MPa}$, the nozzle is perfectly expanded. However, for the present experimental study the gas stagnation pressure $p_{\mathrm{t,g}}$ has been varied in the range of $0.4\,\mathrm{MPa}$ to $1.6\,\mathrm{MPa}$. Consequently, for all relevant set points of operation the gas nozzle has been operated in highly underexpanded condition, leading to complex patterns of compression and expansion waves downstream of the nozzle. An example of these flow patterns is shown on the right in Fig. 1b in the form of a focusing Schlieren image, clearly visualizing strong density gradients in the vertical direction (Luh et al., 2018). Numerical simulations of the gas-only flow for the above mentioned gas stagnation pressures $p_{\mathrm{t,g}}$ have revealed local gas velocities as high as $660\,\mathrm{m\,s^{-1}}$ downstream of the atomizer due to the strong expansion of the gas (Vogl et al., 2019).
Water is supplied to the liquid nozzle by means of a custom pressurized tank, allowing for overpressures of up to $1\,\mathrm{MPa}$. In this manner, freely adjustable liquid mass flow rates of up to $\dot{m}_{\mathrm{l}} = 9\,\mathrm{kg\,min^{-1}}$ can be set with only very minimal fluctuations compared to, for instance, a pump. The outflow is adjusted using a motor driven proportional valve and an external PID controller. This is an important aspect of the present experimental study, since it allows for decoupling the gas and the liquid flow. As has been described by, for instance, Miller et al. (1996), the gas flow can cause a strong underpressure inside of the liquid nozzle, which, however, is also affected by the liquid flow, resulting in a complex coupling. Therefore, without a proper control system, it is usually very difficult to set and maintain a specific set point of operation. In addition, the pressurized tank allows for heating the liquid up to a temperature of $85\,^{\circ}\mathrm{C}$, which can be used for adjusting the liquid properties. Finally, the liquid nozzles themselves are manufactured additively from polyamide powder employing a selective laser sintering process, allowing for flexible modifications to the geometry.
An exemplary still image of the multiphase flow produced by the atomizer is shown on the left in Fig. 1b. As can be seen, the spray is not only strongly affected by the gas flow, but also very dense.

2.2. Phase Doppler measurement system

For the experimental investigation of the atomizer, a dual-mode phase Doppler measurement system has been set up using commercially available components from Dantec Dynamics. It comprises a FlowExplorer DPSS laser transmitter featuring wavelengths of $\lambda_{\mathrm{st}} = 561\,\mathrm{nm}$ for the standard system and $\lambda_{\mathrm{pl}} = 532\,\mathrm{nm}$ for the planar system, a $112\,\mathrm{mm}$ HiDense probe receiver, a Dual PDA detector unit as well as a BSA P60 flow and particle processor. The latter has subsequently been upgraded in order to increase the maximum frequency as well as the maximum bandwidth, which is necessary for investigating the high velocities present in supersonic gas atomization.
Both, transmitter and probe receiver, are mounted on a 3D-traversing system, allowing the measurement volume to be positioned freely within the spray. A schematic illustration of the setup is shown in Fig. 2.

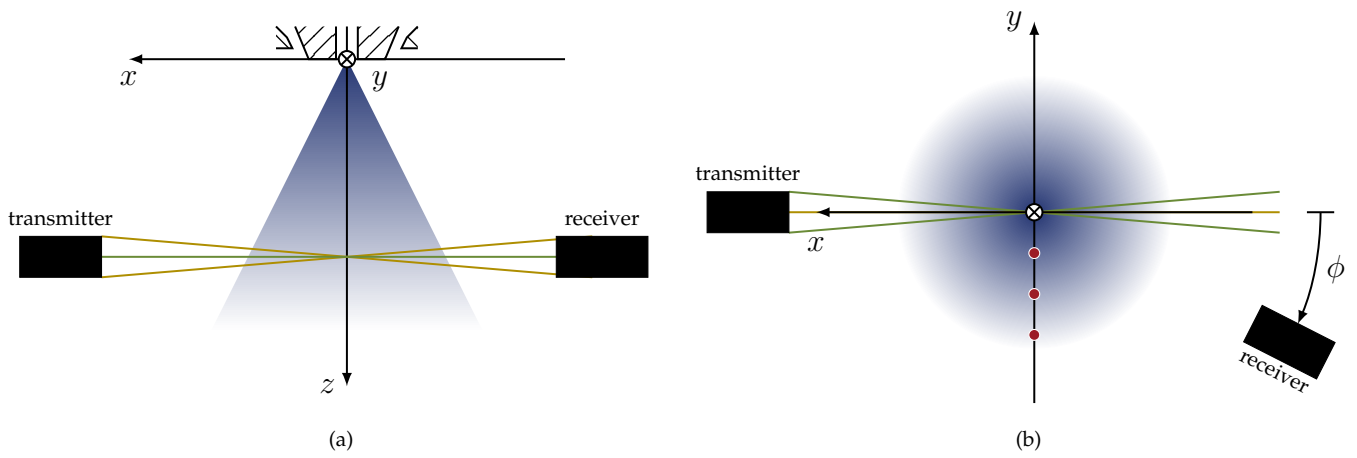

Figure 2. Schematic illustrations of the phase Doppler measurement setup (adapted from Apell et al. (2021)): a) side view, and b) top view (● exemplary measurement position).

The dual-mode system has been employed here, since it not only allows for resolving the 2π-ambiguity and measuring a second particle velocity component, but additionally provides means for assessing the sphericity of measured particles by comparing the orthogonal curvatures measured by the standard and the planar system and, additionally, defining an acceptance band allowing for some tolerable deviation (Tropea et al., 1996). Here, it is important to note that the calculation of the particle diameter d from the measured phase difference $\Delta\Phi$ is solely based on the standard system, which exhibits a higher sensitivity and is less prone to oscillations of the phase-diameter relation for small particles than the planar system (Albrecht et al., 2003). For the same reason, large phase differences $\Delta\Phi$ measured by the planar system are rejected, since they can originate from very small particles resulting in negative phase differences $\Delta\Phi$. This effectively defines a non-acceptance band.

The choice of the optical configuration is a compromise based on the requirements due to the challenging flow conditions present in the spray produced by the supersonic atomizer. For instance, the spray is very dense, making a small measurement volume necessary, in order to avoid multiple particles being present in the measurement volume at the same time. For the available equipment, this is possible by increasing the beam intersection angle Θ and, therefore, reducing the focal length of the transmitter as well as utilizing a small spatial slit filter for the receiving optics, which additionally truncates the measurement volume. However, increasing the beam intersection angle Θ also results in a decreased interference fringe spacing (Albrecht et al., 2003). This is crucial, since particles in the spray have very high velocities, leading in turn to very high measured frequencies. Since both, the maximum bandwidth as well as the maximum frequency of the processor, are limited, a compromise has to be found between reducing the measurement volume and resolving the high particle velocities. Another consequence of the high density of the spray is the choice of the scattering angle ϕ. While the maximum detectable particle diameter needs to be sufficiently large, the scattered light is required to be of sufficient intensity to also reliably detect small particles. Finally, due to the combination of high particle velocities and small measurement volume, the transit times τ of the particles are very short. This is accounted for by setting the sampling rate

of the processor as well as the number of samples per burst accordingly.
In summary, a phase Doppler measurement system has been set up capable of meeting the challenging requirements of sprays produced by a close-coupled atomizer operated with water and air. Here, the maximum particle diameter is $d_{\max} = 107\,\mu\mathrm{m}$ and the maximum particle velocities in axial and radial direction are $u_{z,\max} = 468\,\mathrm{m\,s^{-1}}$ and $u_{r,\max} = 200\,\mathrm{m\,s^{-1}}$, respectively. The system has successfully been applied for the investigation of supersonic gas atomization, achieving average validation and spherical validation rates of about $75\,\%$ and $70\,\%$, respectively, and data rates of up to $20\,\mathrm{kHz}$. Considering the challenges described above, these results are deemed to be satisfactory.

2.3. Experimental methods

Measurements have been performed mainly at an axial distance from the liquid nozzle of $z = 500\,\mathrm{mm}$, where the spray is considered to be fully developed. The radial measurement position r has been varied systematically under the assumption of radial symmetry of the spray in order to characterize the entire spray cross section. As can be seen from the exemplary measurement positions indicated in Fig. 2b, measurements have been restricted to the negative y-axis, that is, $r = -y$. This way, the negative effect of obscuration on the data quality has been reduced. Furthermore, here the influence of the radial particle velocity component is assumed to be minimal and the planar system is used to measure the radial particle velocity component u_r. Here the spray is assumed to be two-dimensional.
For the atomizer configuration described in Section 2.1, a well-defined set point of operation is characterized by the gas stagnation pressure $p_{\mathrm{t,g}}$, which for the choked convergent-divergent nozzle is directly proportional to the gas mass flow rate $\dot{m}_{\mathrm{g}}$, and the liquid mass flow rate $\dot{m}_{\mathrm{l}}$. During this experimental study, neither the gas temperature $T_{\mathrm{t,g}}$ nor the liquid temperature T_{l} has been explicitly adjusted.

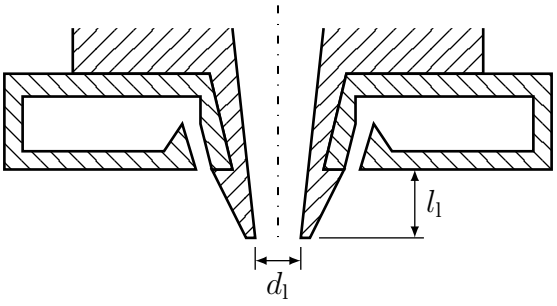

Figure 3. Definition of the liquid nozzle diameter d_{l} as well as the protrusion length l_{l}.

While the focus of this experimental study has been on the influence of the set point of operation on local particle size and velocity distributions, the effect of specific changes to the atomizer design has also been investigated. In detail, two different geometric dimensions have been considered, which are defined in Fig. 3. The liquid nozzle diameter d_{l} is an important parameter, since for gravity-driven atomizers it has a direct influence on the liquid mass flow rate $\dot{m}_{\mathrm{l}}$. Furthermore,

it is used in many empirical correlations employed for predicting the atomization result, like, for instance, the one proposed by Lubanska (1970). Consequently, its effect on the particle size distribution is of great interest. For this experimental study, the baseline liquid nozzle diameter has been $d_\mathrm{l} = 4\,\mathrm{mm}$. Additionally, two other liquid nozzles having diameters of $d_\mathrm{l} = 3\,\mathrm{mm}$ and $d_\mathrm{l} = 5\,\mathrm{mm}$ have been investigated. The influence of the protrusion length l_l, which describes how far the liquid nozzle protrudes into the gas flow field, is less obvious. As has been shown by Wolf and Bergmann (2002), it does affect the underpressure inside of the liquid nozzle caused by the gas flow. Therefore, this geometric dimension provides another means for influencing the liquid mass flow rate $\dot{m}_\mathrm{l}$. Here, the baseline protrusion length has been $l_\mathrm{l} = 6\,\mathrm{mm}$, but two additional liquid nozzles having protrusions lengths of $l_\mathrm{l} = 5\,\mathrm{mm}$ and $l_\mathrm{l} = 7\,\mathrm{mm}$ have been taken into account.

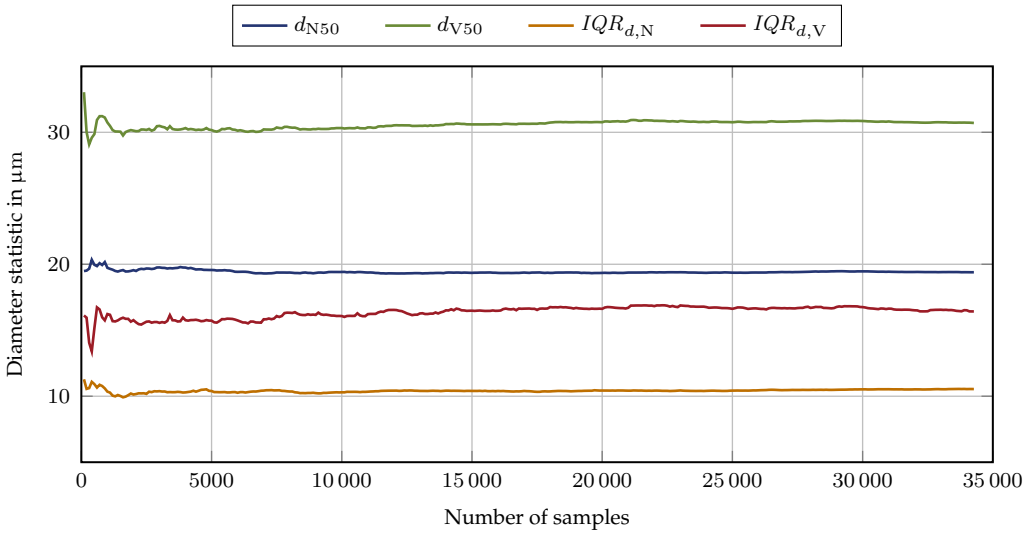

Figure 4. Convergence of relevant particle size statistics with increasing number of validated particles for an exemplary and representative set point of operation.

For each measurement position, at least $20\,000$ validated particles have been recorded. In Fig. 4, the convergence of several relevant particle size statistics with increasing number of validated particles is shown. Here, the set point of operation of the atomizer has been chosen to be representative for the entire experimental study and the particle size statistics have been evaluated every 100 samples. Shown are the number median diameter d_{N50} as well as the volume median diameter d_{V50}. Additionally, as measures of the dispersion of the particle size, the corresponding interquartile ranges $IQR_{d,\mathrm{N}} = d_{\mathrm{N75}} - d_{\mathrm{N25}}$ and $IQR_{d,\mathrm{V}} = d_{\mathrm{V75}} - d_{\mathrm{V25}}$ are shown. As can be seen, all of the statistics converge sufficiently within $15\,000$ validated particles.

2.4. Data processing

Data has been acquired using the upgraded BSA P60 processor in combination with the BSA Flow software 6.5 by Dantec Dynamics. Here, it is important to note that only raw data has been acquired, that is, arrival time t, transit time τ, phase differences $\Delta\Phi$, particle diameter d as well as

particle velocity components in axial and radial direction u_z and u_r, respectively. The actual data evaluation has been done in a subsequent post-processing step using MATLAB software. This includes mainly a retroactive validation, the calculation of particle size and velocity distributions, of statistical corrections and of characteristic particle size and velocity statistics.
In order to account for bias introduced by the phase Doppler measurement principle, two correction methods have been applied. First, since the detection volume is dependent on the particle diameter d and, for receiving optics employing a spatial filter, additionally on the particle trajectory (Albrecht et al., 2003), the number of large particles measured in general is statistically overestimated. This has been corrected for by employing an estimate of the effective diameter of the detection volume based on the burst length following the approach by Tropea and Roisman (2001) and using the weighting factor described by Widmann et al. (2001).

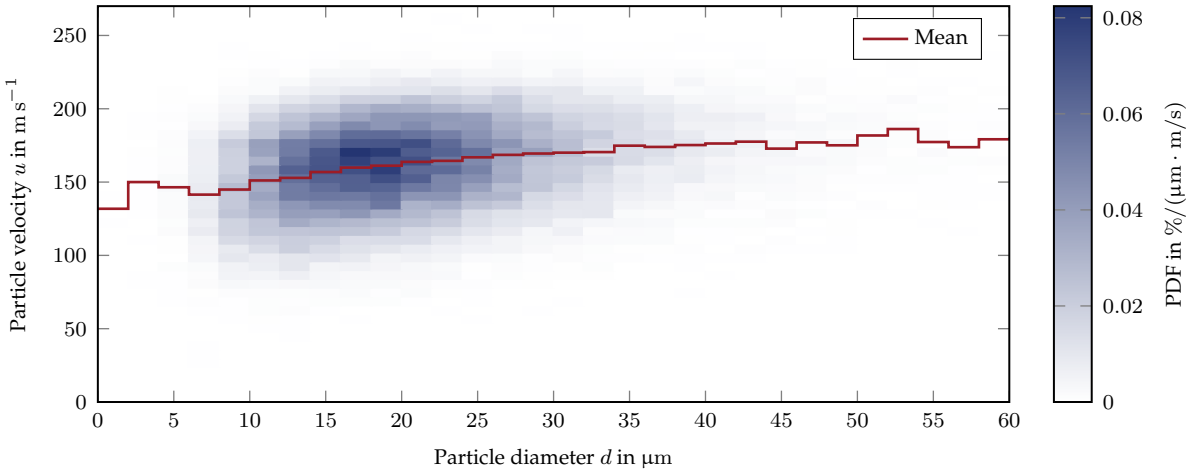

Figure 5. Correlation between particle diameter d and particle velocity u for an exemplary and representative set point of operation.

Second, due to the data rate depending on the particle velocity u, the number of fast particles is generally statistically overestimated. This velocity bias has been accounted for by applying a weighting scheme described by Buchhave et al. (1979). Interestingly, for the spray investigated as part of this experimental study, particle diameter d and particle velocity $u = \left(u_z^2 + u_r^2\right)^{1/2}$ are slightly positively correlated, as can be seen from Fig. 5. Here, the raw data for the particle diameter d and the particle velocity u is shown as a discrete probability density function as well as a mean value for an exemplary and representative set point of operation. Consequently, it is important to correct for the velocity bias, in order to avoid bias in the particle size statistics.
While the data evaluation has been implemented in MATLAB, burst validation and sphericity validation have been performed internally by the processor. Here, it has been observed that, in some cases, the processor validates a fraction of the bursts even though raw data, for instance, arrival time t and transit time τ, indicate the simultaneous presence of two consecutive particles within the measurement volume. The issue has been discussed with Dantec Dynamics and resolved by implementing a suitable filter in the MATLAB evaluation routine.
Finally, as part of the data processing, the measurement uncertainty has been evaluated, which

is a crucial necessity for quantitatively comparing data. Here, two different contributions have been considered and used to calculate a combined standard deviation. First, random fluctuations have been estimated numerically employing the bootstrap resampling method described by Efron and Tibshirani (1994) and $10\,000$ bootstrap samples for each measured distribution. This has been necessary, since the experimental investigation of supersonic atomization is complex and does not allow for repeating each measurement a statistically sufficient number of times.

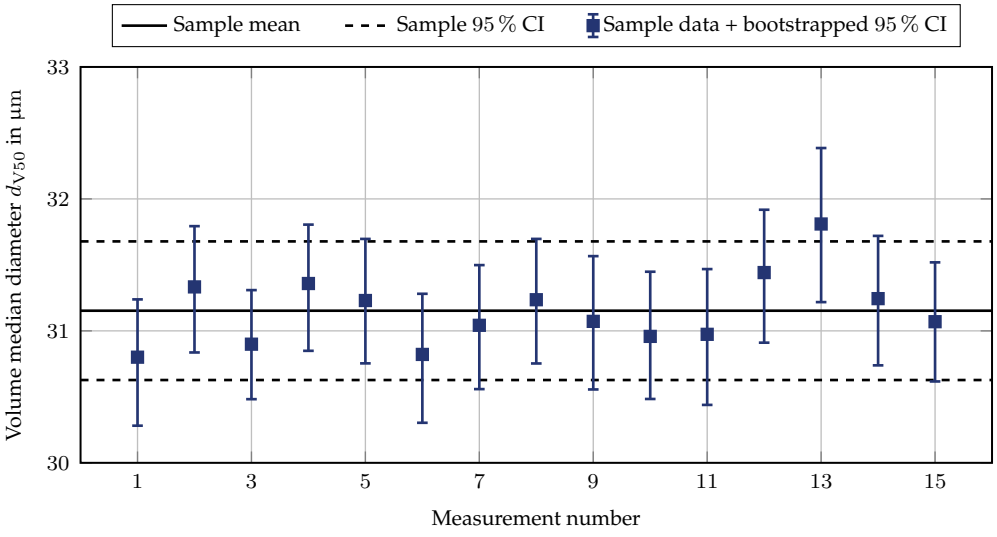

Figure 6. Comparison of measured random fluctuations and $95\,\%$ confidence intervals calculated employing the bootstrap method.

In Fig. 6, results for the volume median diameter d_{V50} for 15 individual measurements at the same representative set point of operation are shown. The measurements have been performed within a short amount of time. Additionally, the sample mean as well as the $95\,\%$ confidence interval calculated from the 15 values are indicated. Furthermore, for each of the individual measurements the bootstrapped $95\,\%$ confidence interval is shown as error bars. As can be seen, the agreement between measured and numerically estimated fluctuations is very good. Therefore, it has been concluded that the bootstrap method provides useful means for reducing the number of necessary measurements.

The second contribution to the measurement uncertainty concerns the dependence of the atomization on the ambient conditions. Due to constraints like, for instance, the open design of the atomization zone, it has not been possible to avoid these fluctuations. Similar problems have been reported by Wolf and Bergmann (2002), noticing a dependence of the gas flow on the ambient pressure. In order to quantify these uncertainties, a total of 15 measurements at the same representative set point of operation have been made over the course of several days. Consequently, an estimate for the corresponding uncertainty has been obtained.

3. Results and discussion

In this section, results for local particle size and velocity distributions are presented and discussed. First, the influence of the set point of operation of the atomizer on the atomization result is identified. Afterwards, the effect of varying the liquid nozzle diameter d_l as well as the liquid nozzle protrusion length l_l is investigated.

3.1. Identification of parameter trends

For this experimental study, the set point of operation of a supersonic atomizer has been considered to be well-defined by the gas stagnation pressure $p_\mathrm{t,g}$ and the liquid mass flow rate $\dot{m}_\mathrm{l}$. Therefore, the main objective has been to investigate the isolated influence of these two parameters on local particle size and velocity distributions. Here, as a baseline case for the atomizer design, a liquid nozzle diameter of $d_\mathrm{l} = 4\,\mathrm{mm}$ and a liquid nozzle protrusion length of $l_\mathrm{l} = 6\,\mathrm{mm}$ have been employed, as has been described in Section 2.3.

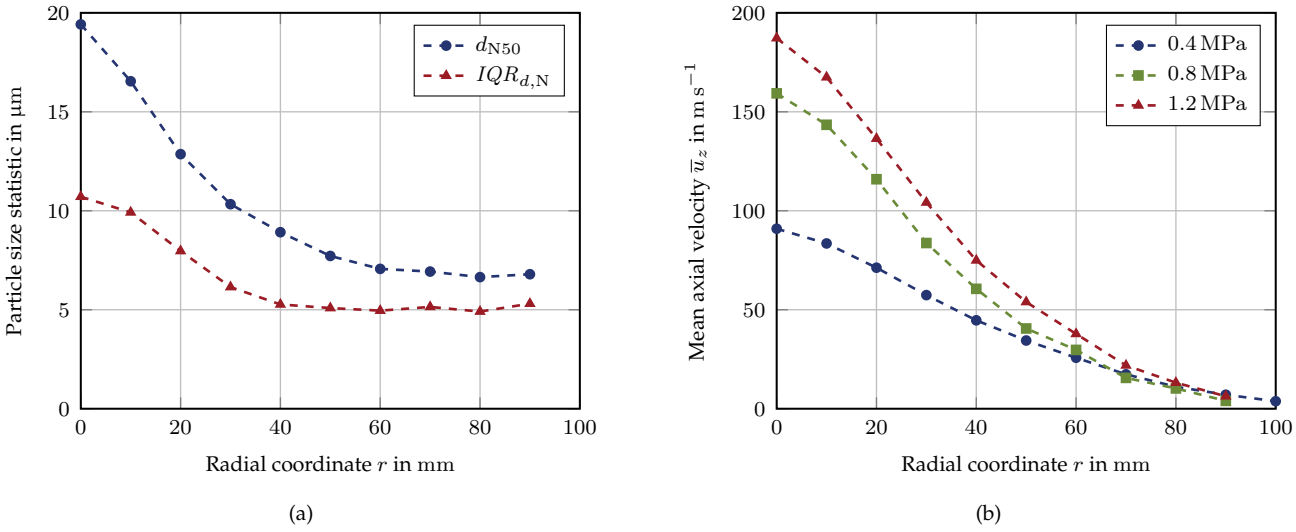

Figure 7. Radial distribution of particle statistics for a liquid mass flow rate of $\dot{m}_\mathrm{l} = 5\,\mathrm{kg\,min^{-1}}$: a) number median diameter d_{N50} and number interquartile range $IQR_{d,\mathrm{N}}$ for a gas stagnation pressure of $p_\mathrm{t,g} = 0.8\,\mathrm{MPa}$, and b) mean axial velocity $\overline{u}_z$ for different constant gas stagnation pressures $p_\mathrm{t,g}$.

To begin with, a few general characteristics of the spray produced by the close-coupled atomizer described in Section 2.1 need to be discussed. In Fig. 7a, radial profiles of the number median diameter d_{N50} as well as the number interquartile range $IQR_{d,\mathrm{N}}$ are shown for a liquid mass flow rate of $\dot{m}_\mathrm{l} = 5\,\mathrm{kg\,min^{-1}}$ and a gas stagnation pressure of $p_\mathrm{t,g} = 0.8\,\mathrm{MPa}$. As can be seen, the number median diameter d_{N50} is largest in the center of the spray and gradually decreases with increasing radial distance. Similarly, the dispersion of the particle size, as characterised by the number interquartile range $IQR_{d,\mathrm{N}}$, is largest in the center of the spray. In the outer region of the spray a lower limit for both, the number median diameter d_{N50} as well as the dispersion of the particle size, is reached. Here, the edge of the spray is defined by a strong decrease in data rate.

These general findings have been found to be consistent for all set points of operation considered. Additionally, in Fig. 7b, radial profiles of the mean axial particle velocity $\overline{u}_z$ for a liquid mass flow rate of $\dot{m}_\mathrm{l} = 5\,\mathrm{kg\,min^{-1}}$ and three different constant gas stagnation pressures $p_\mathrm{t,g}$ are displayed. It is obvious that the gas stagnation pressure $p_\mathrm{t,g}$ has a strong influence on the particle velocity, which is again highest right in the center of the spray and quickly decreases with increasing radial distance. On the other hand, the liquid mass flow rate $\dot{m}_\mathrm{l}$, which is not shown here, only has a small effect on the mean axial particle velocity $\overline{u}_z$. An increasing liquid mass flow rate $\dot{m}_\mathrm{l}$ results in slightly slower particles.
In the following, more detailed analysis, only the center of the spray ($r = 0$) will be considered.

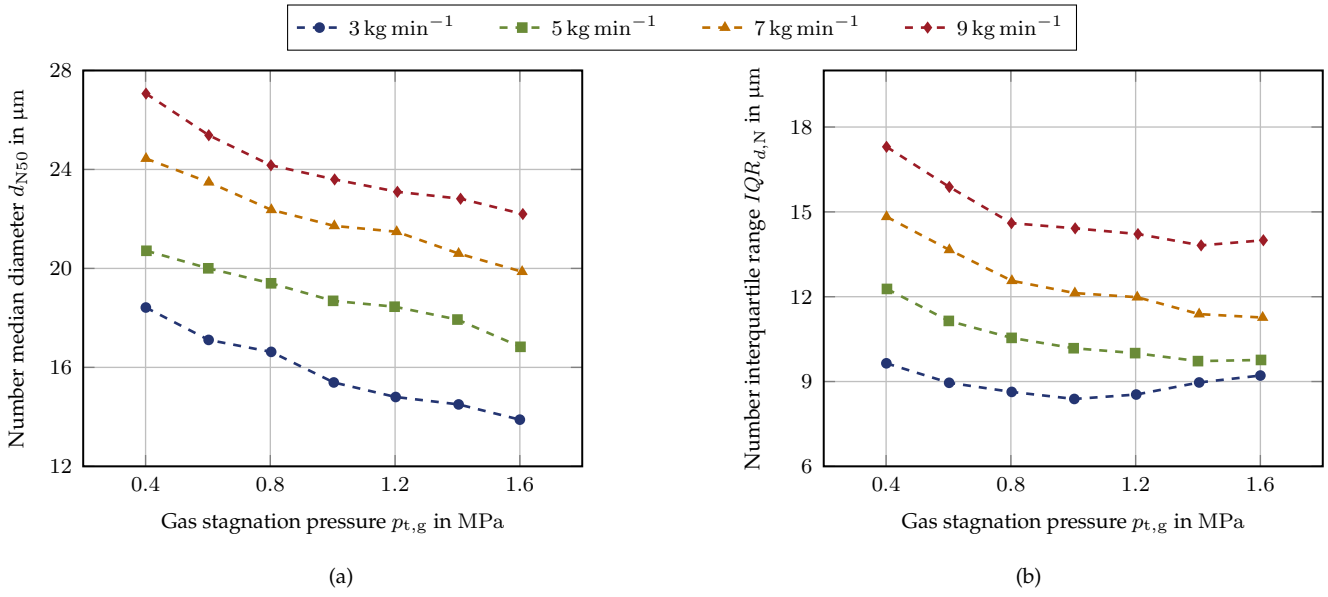

Figure 8. Particle size statistics as a function of the gas stagnation pressure $p_\mathrm{t,g}$ for different constant liquid mass flow rates $\dot{m}_\mathrm{l}$: a) number median diameter d_N50, and b) number interquartile range $IQR_{d,\mathrm{N}}$.

The gas stagnation pressure $p_\mathrm{t,g}$ is the most widely studied operational parameter in the context of supersonic gas atomization, since it is easiest to vary during the actual atomization. Its effect on the number median diameter d_N50 and the number interquartile range $IQR_{d,\mathrm{N}}$ for four different constant liquid mass flow rates $\dot{m}_\mathrm{l}$ is shown in Fig. 8. As can be seen, not only does an increasing gas stagnation pressure $p_\mathrm{t,g}$ reduce the number median diameter d_N50, but it also results in a reduced dispersion of the particle size. Consequently, the gas stagnation pressure $p_\mathrm{t,g}$ provides means for achieving well-defined and narrow particle size distributions. As is obvious from Fig. 8b, there appears to be a lower limit for the number interquartile range $IQR_{d,\mathrm{N}}$. For a very low liquid mass flow rate of $\dot{m}_\mathrm{l} = 3\,\mathrm{kg\,min^{-1}}$, the dispersion of the particle size seems to even increase again for high gas stagnation pressures $p_\mathrm{t,g}$. In general, the results are in good agreement with the findings by, for instance, Urionabarrenetxea et al. (2021).

One of the novel contributions of this experimental study is the systematic investigation of the influence of the liquid mass flow rate $\dot{m}_\mathrm{l}$ on the atomization result. In Fig. 9, the number median diameter d_N50 as well as the number interquartile range $IQR_{d,\mathrm{N}}$ are shown as a function of the liquid mass flow rate $\dot{m}_\mathrm{l}$ for four different constant gas stagnation pressures $p_\mathrm{t,g}$. It can be seen that both

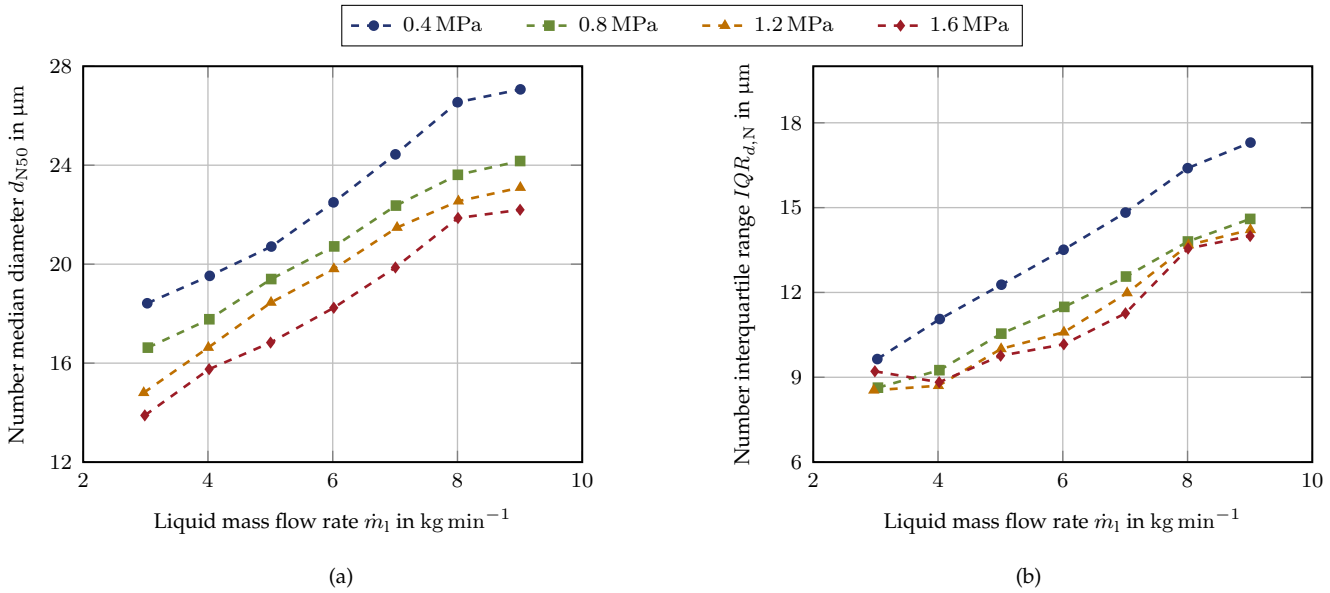

Figure 9. Particle size statistics as a function of the liquid mass flow rates $\dot{m}_l$ for different constant gas stagnation pressures $p_{t,g}$: a) number median diameter d_{N50}, and b) number interquartile range $IQR_{d,N}$.

quantities share a qualitatively similar behavior. That is, increasing the liquid mass flow rate $\dot{m}_l$ not only leads to larger number median diameters d_{N50}, but it also results in an increased dispersion of the particle size. Interestingly, in the parameter range considered here, the atomization result is more sensitive to changes in the liquid mass flow rate $\dot{m}_l$ than in the gas stagnation pressure $p_{t,g}$. This could be a first indicator that, in order to achieve fine-tuned and well-defined atomization results, a control system for the liquid mass flow rate $\dot{m}_l$ is crucial, especially since the atomization gas consumption is a large cost factor.
Finally, one parameter often employed when assessing supersonic gas atomization is the gas-to-liquid ratio $GLR = \dot{m}_g/\dot{m}_l$, which is defined as the ratio of gas and liquid mas flow rate, $\dot{m}_g$ and $\dot{m}_l$, respectively, and can be understood as a measure of the atomization efficiency (Miller et al., 1996). Consequently, the gas-to-liquid ratio GLR is often used in empirical correlations, like, for instance, the one proposed by Lubanska (1970), for predicting the particle size. However, the gas-to-liquid ratio GLR lacks a clear physical meaning, that is, it does not take into account the local gas flow field. Therefore, a more detailed investigation of its influence is necessary.

In Fig. 10, the same data for the particle size statistics already shown in Fig. 9 is displayed again for four different constant gas stagnation pressures $p_{t,g}$, but this time as a function of the gas-to-liquid ratio GLR. Two trends can be identified, which are also widely accepted in the literature (Urionabarrenetxea et al., 2021). First, increasing the gas-to-liquid ratio GLR leads to reduced number median diameters d_{N50} as well as a reduced dispersion of the particle size. Second, there is a lower limit for both particle size statistics. That is, strongly increasing the gas-to-liquid ratio GLR not only is not economically reasonable but also does not improve the atomization result further. Moreover, it is obvious from Fig. 10 that the atomization result cannot be described just by the gas-to-liquid ratio GLR: for identical gas-to-liquid ratios GLR different number median diameters d_{N50} and number interquartile range $IQR_{d,N}$ are achievable, depending on the specific

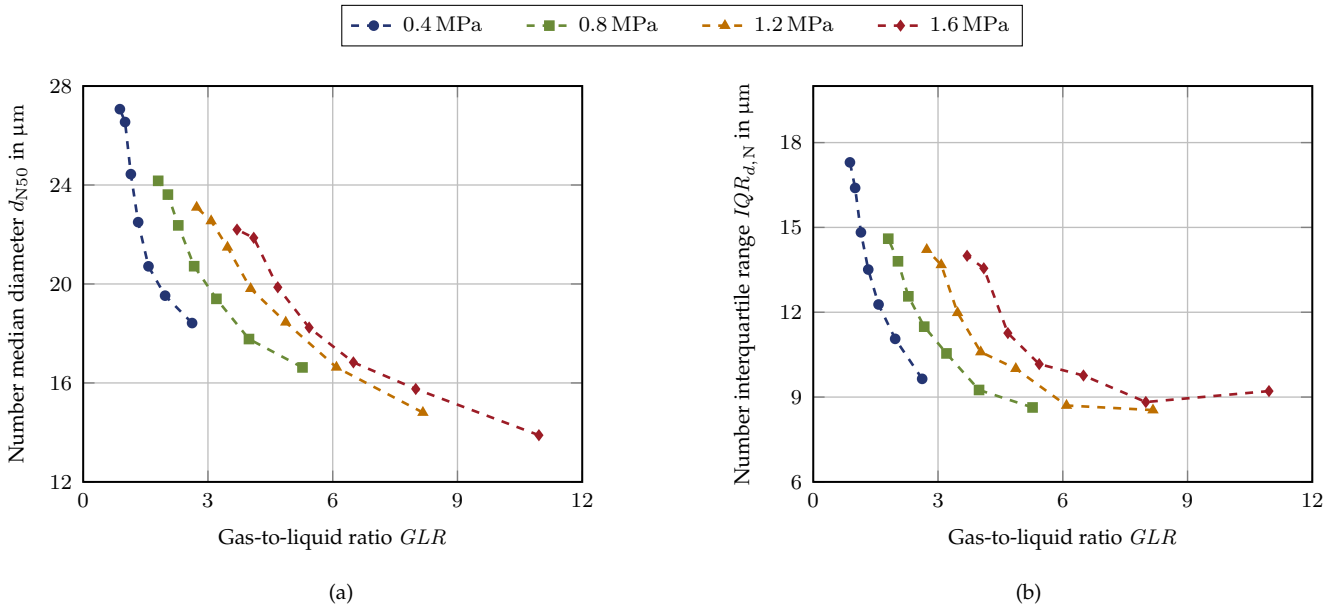

Figure 10. Particle size statistics as a function of the gas-to-liquid ratio GLR for different constant gas stagnation pressures $p_{t,g}$: a) number median diameter d_{N50}, and b) number interquartile range $IQR_{d,N}$.

gas stagnation pressure $p_{t,g}$ and liquid mass flow rate $\dot{m}_l$. This is an important result, especially in the context of modeling, and confirms a recent observation by Urionabarrenetxea et al. (2021), who have identified a clear influence of the gas mass flow rate $\dot{m}_g$. Interestingly, however, they have found a decreasing particle size with increasing gas mass flow rate $\dot{m}_g$ for constant gas-to-liquid ratios GLR. In contrast, as can be seen in Fig. 10a, here the effect is the opposite, due to the strong influence of the liquid mass flow rate $\dot{m}_l$ discussed above. This strongly suggests that a clear understanding of the local gas flow is crucial for describing the atomization process, while global quantities like the gas-to-liquid ratio GLR can be misleading.

3.2. Influence of the liquid nozzle diameter

As has been described in Section 2.3, the liquid nozzle diameter d_l usually has a direct effect on the liquid mass flow rate $\dot{m}_l$. Therefore, it is of interest to isolate its influence on the atomization result by comparing results for different liquid nozzle diameters d_l but identical liquid mass flow rates $\dot{m}_l$. This has been possible due to the control system mentioned in Section 2.1. In detail, three different liquid nozzle diameters d_l ($3\,\mathrm{mm}$, $4\,\mathrm{mm}$ and $5\,\mathrm{mm}$) have been considered.

In order to compare atomization results for the three different liquid nozzle diameters d_l, in Fig. 11a the number median diameter d_{N50} is shown as a function of the gas stagnation pressure $p_{t,g}$ for a liquid mass flow rate of $\dot{m}_l = 5\,\mathrm{kg\,min^{-1}}$. The data is representative for the entire parameter range, which has been considered. Interestingly, differences between the three nozzles are very small. In fact, when investigating the actual differences between the modified liquid nozzles ($3\,\mathrm{mm}$ and $5\,\mathrm{mm}$) and the baseline case ($4\,\mathrm{mm}$) and also considering the measurement uncertainty, characterized by $95\,\%$ confidence intervals, which are both shown in Fig. 11b, it can be concluded that no

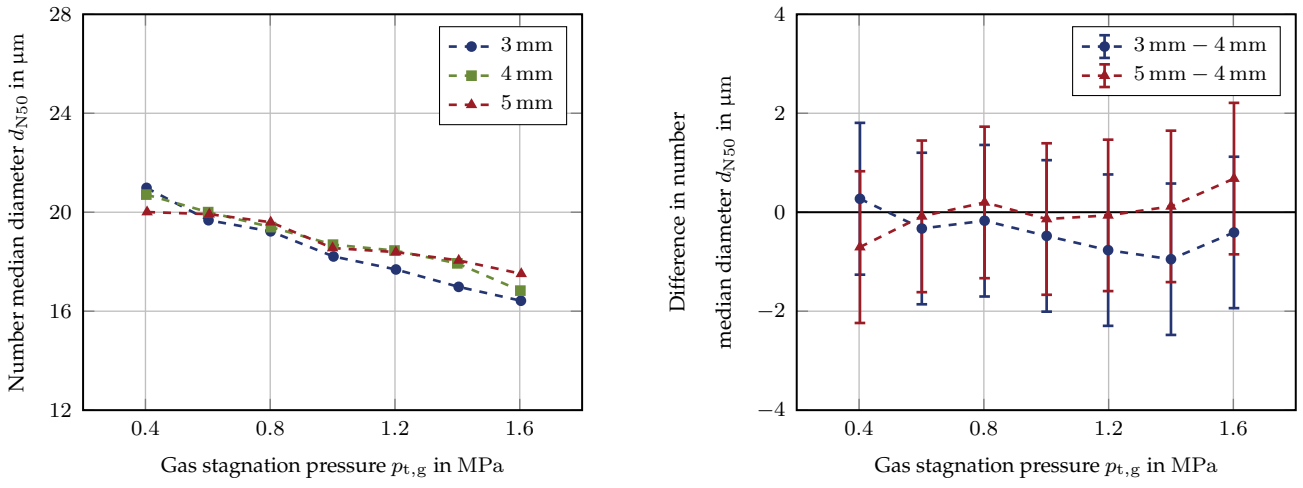

(a) (b)

Figure 11. Influence of the liquid nozzle diameter d_l as a function of the gas stagnation pressure $p_{t,g}$ for a liquid mass flow rate of $\dot{m}_l = 5\,\mathrm{kg\,min^{-1}}$ on: a) number median diameter d_{N50}, and b) difference in number median diameter d_{N50}.

significant influence of the liquid nozzle diameter d_l on the number median diameter d_{N50} can be observed. This is an important result, which needs to be considered when trying to model the particle size produced by supersonic gas atomization. Additionally, in combination with the results shown above in Fig. 9a, this confirms that it is indeed the liquid mass flow rate $\dot{m}_l$ and not the liquid exit velocity u_l, which affects the number median diameter d_{N50} most significantly.

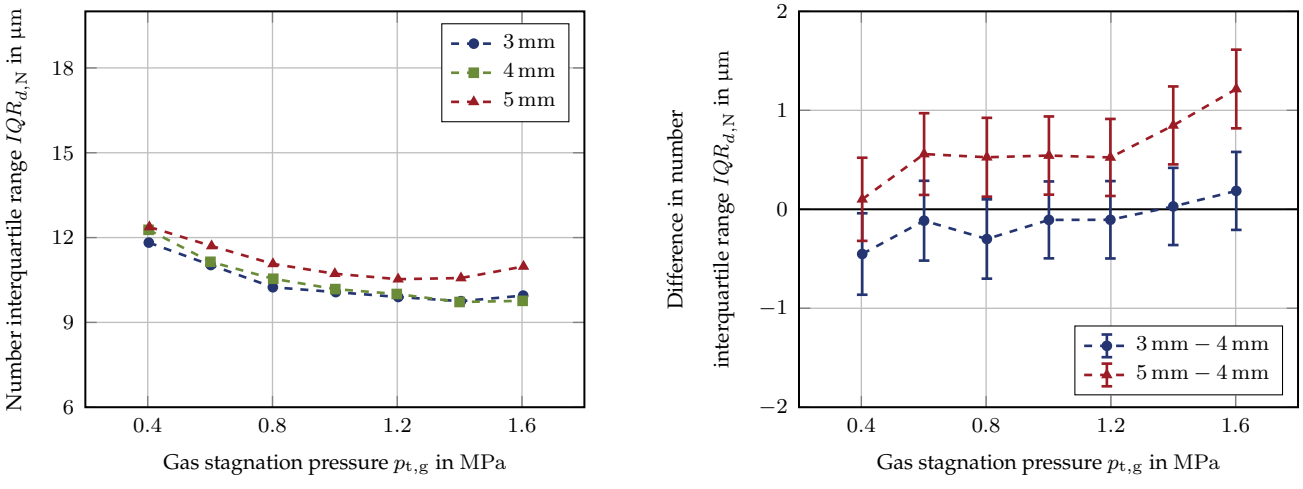

(a) (b)

Figure 12. Influence of the liquid nozzle diameter d_l as a function of the gas stagnation pressure $p_{t,g}$ for a liquid mass flow rate of $\dot{m}_l = 5\,\mathrm{kg\,min^{-1}}$ on: a) number interquartile range $IQR_{d,N}$, and b) difference in number interquartile range $IQR_{d,N}$.

Using the same approach as above for the number median diameter d_{N50}, in Fig. 12 the effect of the liquid nozzle diameter d_l on the number interquartile range $IQR_{d,N}$ is compared. Again, the influence appears to be small. However, in contrast to the discussion above, a significant difference can be seen for the combination of high gas stagnation pressures $p_{t,g}$ and the liquid nozzle diameter

of $d_\mathrm{l} = 5\,\mathrm{mm}$ in Fig. 12b. The dispersion of the particle size is slightly greater when compared to the results of the liquid nozzle diameter of $d_\mathrm{l} = 4\,\mathrm{mm}$.
In the context of metal atomization, the liquid nozzle diameter of d_l is often increased in order to avoid freezing of the liquid nozzle due to the very low temperature of the expanding gas flow. For gravity driven atomizers, however, this has direct consequences for the atomization result, as can be seen from the results discussed above. More specifically, increasing the liquid nozzle diameter d_l leads to increased liquid mass flow rates $\dot{m}_\mathrm{l}$ and, in turn, for constant gas stagnation pressure $p_\mathrm{t,g}$, to larger number median diameters d_N50 and an increased dispersion of the particle size.

3.3. Influence of the liquid nozzle protrusion length

As a second variation to the baseline atomizer geometry, the liquid nozzle protrusion length l_l has been varied ($5\,\mathrm{mm}$, $6\,\mathrm{mm}$ and $7\,\mathrm{mm}$) and examined using the same approach already introduced for the liquid nozzle diameter in Section 3.2. The baseline case has been the liquid nozzle protrusion length of $l_\mathrm{l} = 6\,\mathrm{mm}$.
The liquid nozzle protrusion length l_l is an interesting parameter, since it determines how the liquid interacts first with the expanding gas flow. Therefore, it is likely that its influence is highly dependent on the actual atomizer design. This has to be noted when interpreting the results discussed below.

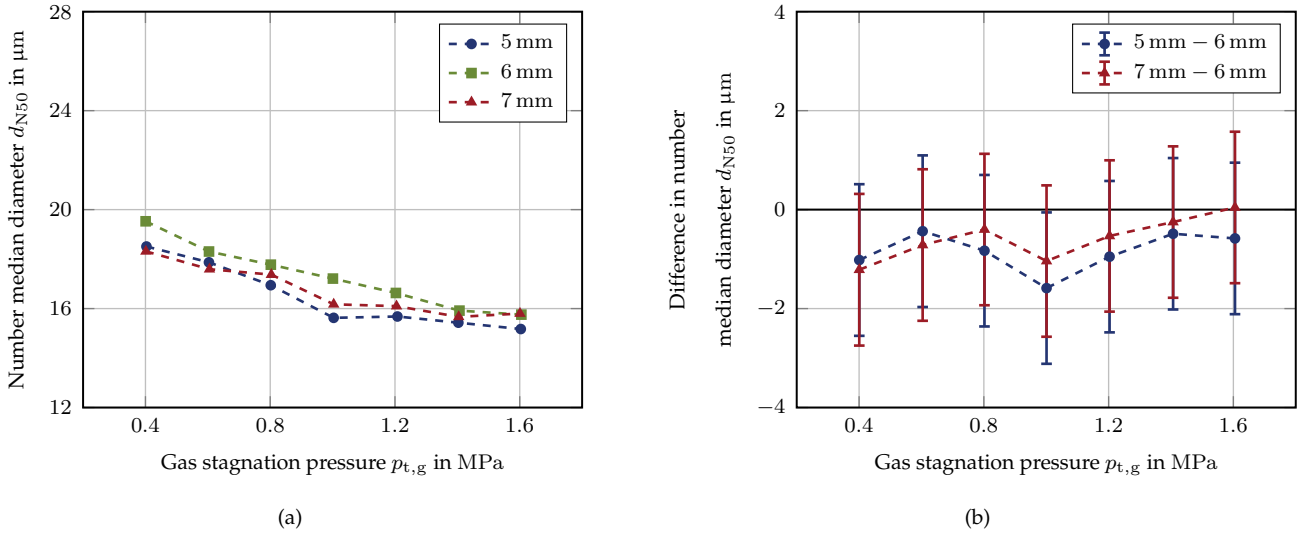

Figure 13. Influence of the liquid nozzle protrusion length l_l as a function of the gas stagnation pressure $p_\mathrm{t,g}$ for a liquid mass flow rate of $\dot{m}_\mathrm{l} = 4\,\mathrm{kg\,min^{-1}}$ on: a) number median diameter d_N50, and b) difference in number median diameter d_N50.

In Fig. 13 the influence of the liquid nozzle protrusion length l_l on the number median diameter d_N50 is investigated as a function of the gas stagnation pressure $p_\mathrm{t,g}$. Here, the data is shown for a constant liquid mass flow rate of $\dot{m}_\mathrm{l} = 4\,\mathrm{kg\,min^{-1}}$. While the baseline case ($6\,\mathrm{mm}$) has been found to result in the largest number median diameters d_N50, analysis of the actual differences and the corresponding measurement uncertainties shows that no significant effect has been observed.

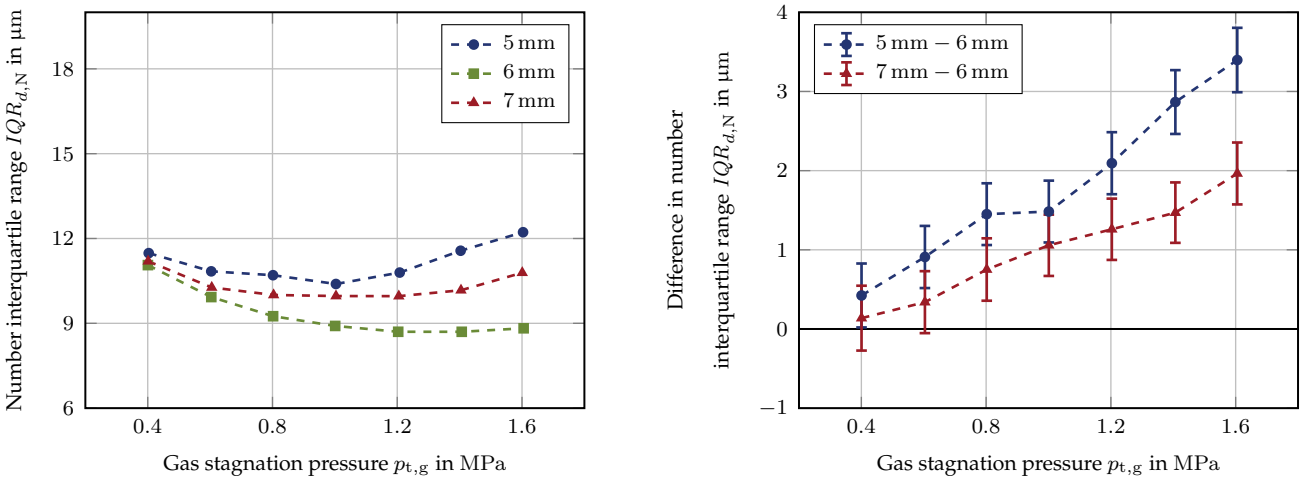

Figure 14. Influence of the liquid nozzle protrusion length l_l as a function of the gas stagnation pressure $p_{t,g}$ for a liquid mass flow rate of $\dot{m}_l = 4\,\mathrm{kg\,min^{-1}}$ on: a) number interquartile range $IQR_{d,N}$, and b) difference in number interquartile range $IQR_{d,N}$.

In contrast, a clear difference in number interquartile range $IQR_{d,N}$ is obvious from Fig. 14a. For increasing gas stagnation pressure $p_{t,g}$, both of the modified liquid nozzles ($5\,\mathrm{mm}$ and $7\,\mathrm{mm}$) result in a larger dispersion of the particle size compared to the baseline case ($6\,\mathrm{mm}$). This is emphasized by the actual differences shown in Fig. 14b. Interestingly, the results do not allow for stating a clear trend. Consequently, it can be concluded that liquid nozzle design and gas flow need to be precisely tuned in order to optimize the atomization result.

For the atomizer design used as part of this experimental study, the liquid nozzle protrusion length l_l has been found to have a strong influence on the liquid mass flow rate $\dot{m}_l$. While these results are not discussed in the scope of this work, it is worth noting that this is in agreement with the findings by Wolf and Bergmann (2002). As a result, the data discussed above indicates that while the liquid nozzle protrusion length l_l can be used to adjust the liquid mass flow rate $\dot{m}_l$, this again has direct consequences for the number median diameter d_{N50} as well as the number interquartile range $IQR_{d,N}$, emphasizing the complex coupling of atomizer geometry and operational parameters existing for supersonic gas atomization.

4. Summary and Conclusions

A dual-mode phase Doppler measurement system has been set up for the characterization of the spray produced by a supersonic close-coupled atomizer operated with water and air. The system has been successfully used for the systematic investigation of the influence of the gas stagnation pressure $p_{t,g}$ and the liquid mass flow rate $\dot{m}_l$ on local particle size and velocity distributions. Additionally, the effect of the liquid nozzle diameter d_l as well as the liquid nozzle protrusion length l_l have been studied briefly.

An increase in the gas stagnation pressure $p_{t,g}$ has been found to result in a reduced number me-

dian diameter d_{N50}. Similarly, this increase leads to a decreased number interquartile range $IQR_{d,\mathrm{N}}$, i.e. dispersion of the particle size. However, the sensitivity decreases. These results are in accordance with typical findings from the literature, which indicates the suitability of the phase Doppler measurement technology for the characterization of supersonic gas atomization.
As a novel approach in this study, the liquid mass flow rate $\dot{m}_{\mathrm{l}}$ has been precisely controlled during the atomization process, allowing for a systematic assessment of its influence on the particle size. The liquid mass flow rate $\dot{m}_{\mathrm{l}}$ has been identified to be an important parameter determining the atomization result. In detail, both the number median diameter d_{N50} and the number interquartile range $IQR_{d,\mathrm{N}}$ increase with increasing liquid mass flow rate $\dot{m}_{\mathrm{l}}$. In fact, the atomization result has been found to be more sensitive to changes in the liquid mass flow rate $\dot{m}_{\mathrm{l}}$ than in the gas stagnation pressure $p_{\mathrm{t,g}}$.
Furthermore, the data obtained at well-defined set points of operation has been used to study the dependence of the atomization result on the gas-to-liquid ratio GLR. This dependence has been shown to be ambiguous in the sense that, for a specific gas-to-liquid ratio GLR, neither the number median diameter d_{N50} nor the number interquartile range $IQR_{d,\mathrm{N}}$ is uniquely determined, but remains a function of the gas stagnation pressure $p_{\mathrm{t,g}}$ and the liquid mass flow rate $\dot{m}_{\mathrm{l}}$. Considering that the gas-to-liquid ratio GLR is often employed in empirical models to predict the particle size, this is an important conclusion.
Finally, while neither the liquid nozzle diameter d_{l} nor the liquid nozzle protrusion length l_{l} has been found to affect the number median diameter d_{N50}, for increasing gas stagnation pressure $p_{\mathrm{t,g}}$, the number interquartile range $IQR_{d,\mathrm{N}}$ does indeed depend strongly on the liquid nozzle protrusion length l_{l} and at least slightly on the liquid nozzle diameter d_{l}. This, again, emphasizes the difficult coupling between operational parameters and the atomizer geometry arising in supersonic gas atomization.
Future work will focus on gaining more insight into the local flow field, the primary atomization mechanism and the gas-liquid interfaces, in order to improve the understanding of how operational parameters and the specific geometric atomizer design influence the atomization process.

Acknowledgements

The authors gratefully acknowledge the Indo-German Science & Technology Centre (IGSTC) for the financial support of the project "Metal Powder Production for Additive Manufacturing" (PPAM), funding code 01DQ19005A.

Nomenclature

λ_{pl}	Wavelength of the planar system [m]
λ_{st}	Wavelength of the standard system [m]
ϕ	Scattering angle [°]

$\Delta\Phi$	Phase difference [°]
ϱ_g	Gas density [$\mathrm{kg\,m^{-3}}$]
τ	Transit time [s]
Θ	Beam intersection angle [°]
d	Particle diameter [m]
d_l	Liquid nozzle diameter [m]
d_max	Maximum particle diameter [m]
d_N50	Number median diameter [m]
d_V50	Volume median diameter [m]
GLR	Gas-to-liquid ratio [$-$]
$IQR_{d,\mathrm{N}}$	Number interquartile range [m]
$IQR_{d,\mathrm{V}}$	Volume interquartile range [m]
l_l	Liquid nozzle protrusion length [m]
$\dot{m}_\mathrm{g}$	Gas mass flow rate [$\mathrm{kg\,s^{-1}}$]
$\dot{m}_\mathrm{l}$	Liquid mass flow rate [$\mathrm{kg\,s^{-1}}$]
Ma	Mach number [$-$]
$p_\mathrm{t,g}$	Gas stagnation pressure [Pa]
r	Radial coordinate [m]
t	Arrival time [s]
T_l	Liquid temperature [°C]
$T_\mathrm{t,g}$	Gas temperature [°C]
u	Particle velocity [$\mathrm{m\,s^{-1}}$]
u_l	Liquid exit velocity [$\mathrm{m\,s^{-1}}$]
u_r	Radial particle velocity [$\mathrm{m\,s^{-1}}$]
$u_{r,\mathrm{max}}$	Maximum radial particle velocity [$\mathrm{m\,s^{-1}}$]
u_z	Axial particle velocity [$\mathrm{m\,s^{-1}}$]
$\overline{u}_z$	Mean axial particle velocity [$\mathrm{m\,s^{-1}}$]
$u_{z,\mathrm{max}}$	Maximum axial particle velocity [$\mathrm{m\,s^{-1}}$]
x, y, z	Cartesian coordinates [m]

References

Aksoy, A., & Ünal, R. (2006). Effects of gas pressure and protrusion length of melt delivery tube on powder size and powder morphology of nitrogen gas atomised tin powders. *Powder Metallurgy*, *49*(4), 349–354. https://doi.org/10.1179/174329006X89425

Albrecht, H.-E., Borys, M., Tropea, C., & Damaschke, N. (2003). *Laser doppler and phase doppler measurement techniques*. Springer. https://doi.org/10.1007/978-3-662-05165-8

Allimant, A., Planche, M. P., Bailly, Y., Dembinski, L., & Coddet, C. (2009). Progress in gas atomization of liquid metals by means of a de laval nozzle. *Powder Technology*, *190*(1-2), 79–83. https://doi.org/10.1016/j.powtec.2008.04.071

Anderson, I. E., & Terpstra, R. L. (2002). Progress toward gas atomization processing with increased uniformity and control. *Materials Science & Engineering A*, *326*(1), 101–109. https://doi.org/10.1016/S0921-5093(01)01427-7

Antipas, G. S. E. (2011). Liquid column deformation and particle size distribution in gas atomization. *International Journal of Computational Materials Science and Surface Engineering*, *4*, 247–264. https://doi.org/10.1504/IJCMSSE.2011.042822

Apell, N., Tropea, C., Roisman, I. V., & Hussong, J. (2021). Experimental investigation of a close-coupled atomizer using the phase doppler measurement technique. In Institute for Liquid Atomization and Spray Systems (Ed.), *Proceedings of the 15th international conference on liquid atomization & spray systems* (p. 96). https://doi.org/10.2218/iclass.2021.5856

Buchhave, P., George, W. K., & Lumley, J. L. (1979). The measurement of turbulence with the laser-doppler anemometer. *Annual Review of Fluid Mechanics*, *11*(1), 443–503. https://doi.org/10.1146/annurev.fl.11.010179.002303

Domnick, J., Raimann, J., Schutte, K., & Wolf, G. (1998). Phase doppler anemometry in inert and liquid gas atomization. *Atomization and Sprays*, *8*(5), 521–546. https://doi.org/10.1615/AtomizSpr.v8.i5.30

Domnick, J., Raimann, J., Wolf, G., Berlemont, A., & Cabot, M.-S. (1997). On-line process control in melt spraying using phase-doppler anemometry. *International Journal of Fluid Mechanics Research*, *24*(4-6), 694–706. https://doi.org/10.1615/InterJFluidMechRes.v24.i4-6.250

Efron, B., & Tibshirani, R. (1994). *An introduction to the bootstrap* (Vol. 57). Chapman & Hall. https://doi.org/10.1201/9780429246593

Henein, H., Uhlenwinkel, V., & Fritsching, U. (Eds.). (2017). *Metal sprays and spray deposition*. Springer International Publishing. https://doi.org/10.1007/978-3-319-52689-8

Lubanska, H. (1970). Correlation of spray ring data for gas atomization of liquid metals. *JOM*, *22*(2), 45–49. https://doi.org/10.1007/BF03355938

Luh, M. F., Vogl, N., Odenthal, H.-J., Roisman, I. V., & Tropea, C. (2018). Focusing schlieren imaging in close-coupled atomization: Comparison of experimental results with numerical simulations. In Institute for Liquid Atomization and Spray Systems (Ed.), *Proceedings of the 14th international conference on liquid atomization & spray systems* (p. 390).

Mates, S. P., & Settles, G. S. (2005). A study of liquid metal atomization using close-coupled nozzles: Atomization behavior: Part ii. *Atomization and Sprays*, *15*(1), 41–59. https://doi.org/10.1615/AtomizSpr.v15.i1.30

Miller, R. S., Miller, S. A., Savkar, S. D., & Mourer, D. P. (1996). Two phase flow model for the close-coupled atomization of metals. *International Journal of Powder Metallurgy*, *32*(4), 341–352.

Tropea, C., & Roisman, I. V. (2001). Flux measurements in sprays using phase doppler techniques. *Atomization and Sprays*, *11*(6), 34. https://doi.org/10.1615/AtomizSpr.v11.i6.50

Tropea, C., Xu, T.-H., Onofri, F., Géhan, G., Haugen, P., & Stieglmeier, M. (1996). Dual-mode phase-doppler anemometer. *Particle & Particle Systems Characterization*, *13*(2), 165–170. https://doi.org/10.1002/ppsc.19960130216

Ünal, R. (2006). The influence of the pressure formation at the tip of the melt delivery tube on tin powder size and gas/melt ratio in gas atomization method. *Journal of Materials Processing Tech*, *180*(1-3), 291–295. https://doi.org/10.1016/j.jmatprotec.2006.06.018

Ünal, R. (2007a). Improvements to close coupled gas atomisation nozzle for fine powder production. *Powder Metallurgy*, *50*(1), 66–71. https://doi.org/10.1179/174329007X164899

Ünal, R. (2007b). Investigation on metal powder production efficiency of new convergent divergent nozzle in close coupled gas atomisation. *Powder Metallurgy*, *50*(4), 302–306. https://doi.org/10.1179/174329007X189595

Ünal, R., & Aydın, M. (2007). High efficient metal powder production by gas atomisation process. *Materials Science Forum - MATER SCI FORUM*, *534-536*. https://doi.org/10.4028/www.scientific.net/MSF.534-536.57

Urionabarrenetxea, E., Avello, A., Rivas, A., & Martín, J. M. (2021). Experimental study of the influence of operational and geometric variables on the powders produced by close-coupled gas atomisation. *Materials & Design*, *199*, 109441. https://doi.org/10.1016/j.matdes.2020.109441

Vogl, N., Odenthal, H.-J., Hüllen, M., Luh, M., Roisman, I. V., & Tropea, C. (2019). Physical and numerical modeling of close-coupled atomization processes for metal powder production. In Steel Institute VDEh (Ed.), *Proceedings of the 4th european steel technology and application days*.

Widmann, J. F., Presser, C., & Leigh, S. (2001). Improving phase doppler volume flux measurements in low data rate applications. *Measurement Science and Technology*, *12*, 1180–1190. https://doi.org/10.1088/0957-0233/12/8/327

Wolf, G., & Bergmann, H. W. (2002). Investigations on melt atomization with gas and liquefied cryogenic gas. *Materials Science & Engineering A*, *326*(1), 134–143. https://doi.org/10.1016/S0921-5093(01)01433-2